79-4048

Higher-Order Differential Equations of Radiative Transfer: P_3 Approximation

Yildiz Bayazitoğlu* and James Higenyi†
Rice University, Houston, Tex.

The boundary conditions to be used in the P_3 approximation of the spherical harmonics method of the radiative transfer are formulated. The series expansion of the angular distribution of radiative intensity needed by the boundary conditions is extended to include the number of terms in the P_3 approximation. This expansion is given for three-dimensional radiative transfer and the coefficients are determined in terms of the moments of radiation intensity. Although in this whole procedure tedious algebra is required, the final equations of the greatest importance are very convenient to use. The governing differential equations and the obtained boundary conditions for the P_3 approximation are used to solve the radiation exchange for the case of the participating medium between plane parallel plates, concentric cylinders, and concentric spheres.

I. Introduction

THE exact treatment of radiative transfer in participating media results in integrodifferential equations. Mathematically, it is very difficult to work with these equations. Even for idealized situations and simple boundary conditions, solutions are complicated. In the case of engineering applications, the transport of energy within a fluid by radiation, conduction, and/or convection may become equally significant, and their interaction alters the temperature distribution in the medium making the analysis additionally complicated. Therefore, various approximate methods have been developed. Among these, the spherical harmonics method, the moment method, and the discrete ordinate method provide means to obtain higher-order approximate solutions to the equation of radiative transfer. These theories were originally developed for astrophysical studies and were later employed in neutron transport theory and in classical gasdynamics. The approximate governing equations for these studies are similar, but the physical boundary conditions turn out to be different.

The spherical harmonics method was first suggested by Jeans.[1] The radiation intensity is expanded in a series of normalized spherical harmonics:

$$I(r,\Omega)=\sum_{\ell=0}^{\infty}\sum_{m=-\ell}^{\ell}A_\ell^m(r)\,Y_\ell^m(\Omega) \tag{1}$$

where $A_\ell^m(r)$ is a function to be determined and $Y_\ell^m(\Omega)$ is the normalized spherical harmonics:

$$Y_\ell^m(\Omega)=\left[\frac{2\ell+1}{4\pi}\frac{(\ell-m)!}{(\ell+m)!}\right]^{1/2}e^{im\theta}P_\ell^m(\cos\beta) \tag{2}$$

and $P_\ell^m(\cos\beta)$ terms are the associated Legendre polynomials of the first kind.

Equation (1) is cut off arbitrarily after a certain number of terms. The P_n approximation follows when one terminates this series after a certain number of terms. For the P_1 approximation, one lets $A_\ell^m=0$ for $\ell\geq 2$; for the P_3 approximation, one lets $A_\ell^m=0$ for $\ell\geq 4$.

Received June 14, 1978; revision received Sept. 19, 1978.

Index categories: Radiation and Radiative Heat Transfer; Atmospheric and Space Sciences; Combustion and Combustor Designs.

*Assistant Professor, Mechanical Engineering Dept.
†Graduate Student, Mechanical Engineering Dept.

Among the works related to neutron transport theory, Mark[2] and Marshak[3] proposed two different boundary condition approximations for the spherical harmonics method. Later works indicate that Marshak's boundary conditions are generally better than Mark's.[4,5]

The moment method is described by Krook.[6] He also shows that the spherical harmonics method, the discrete ordinate method, and the moment method are equivalent. He demonstrates his arguments by reference to the problem of a plane-stratified gray atmosphere in radiative equilibrium, and shows the relations between these methods in the Eddington approximation. Obviously, the first three moments of the specific intensity I involved in the Eddington approximation have physical significance. In other words, I_0, the first moment of intensity divided by the speed of light, gives the radiation energy density; I_i, the second moment of intensity, is the radiative energy flux in the ith coordinate direction; and I_{ij}, which is the third moment of intensity divided by the speed of light, can be shown to be the radiation stress. The closing condition for the first-moment approximation is $I_{ij}=I_0\delta_{ij}/3$. The treatment of the first-moment approximation, which is also the P_1 approximation, can be found in Siegel and Howell[7] and Özisik.[8]

Assuming that the radiating gas is in local thermodynamic equilibrium, the basic radiation transport equation for the gray gas is:

$$\frac{1}{c}\frac{\partial I}{\partial t}+\ell_i\frac{\partial I}{\partial x_i}=\alpha(E_b/\pi-I) \tag{3}$$

where I is the intensity of radiation, c is the speed of light, α is the volumetric absorption coefficient, E_b is the black-body emissive power, and ℓ_i is the direction cosine in the direction of Cartesian coordinate x_i.

The moment equations are obtained by multiplying the radiative transport, Eq. (3), by powers of the direction cosines, and integrating the result over the complete range of solid angle, noting that emissive power is independent of solid angle. The zeroth-order moment equation is:

$$\frac{\partial I_i}{\partial x_i}=\alpha[4E_b-I_0] \tag{4}$$

where

$$I_0(r)=\int_\Omega I(r,\Omega)\,d\Omega \qquad I_i(r)=\int_\Omega \ell_i I(r,\Omega)\,d\Omega \tag{5}$$

and $E_b = \sigma T^4$. In the integration of Eq. (3), the term $\partial I/c\partial t$ is neglected since it is always smaller than other terms. Multiplying Eq. (3) by ℓ_i and integrating yields the first-order moment equation:

$$\frac{\partial I_{ij}}{\partial x_j} = -\alpha I_i \quad i = 1,2,3 \tag{6}$$

where

$$I_{ij}(r) = \int \ell_i \ell_j I(r,\Omega) d\Omega \tag{7}$$

This procedure can be continued as:

$$\frac{\partial I_{ijk}}{\partial x_k} = -\alpha\left[\frac{4}{3} E_b \delta_{ij} - I_{ij}\right] \tag{8}$$

$$\frac{\partial I_{ijk\ell}}{\partial x_\ell} = -\alpha I_{ijk} \tag{9}$$

$$\vdots$$

where

$$I_{ijk}(r) = \int \ell_i \ell_j \ell_k I(r,\Omega) d\Omega \tag{10}$$

$$I_{ijk\ell}(r) = \int \ell_i \ell_j \ell_k \ell_\ell I(r,\Omega) d\Omega \tag{11}$$

$$\vdots \qquad \vdots$$

The cutoff condition will provide the "closing condition," which will make the preceding set of equations determinate.

The utility of the previously mentioned higher-order differential approximations (spherical harmonic, discrete ordinate, and moment) which prove to result in the same governing equation will be restricted by their accuracy. Spiegel[9] obtained an exact solution to the radiative relaxation problem for small thermat perturbations imposed on an isothermal medium. When the results are compared with the Eddington approximation used in the solution of the problem, they differ around moderate optical thicknesses (Unno and Spiegel[10]). In addition to the preceding problem, Arpaci and Gözüm[11] compared the results of P_1, P_3, and P_5 approximations with Spiegel's[12] exact solution to the Benard problem in which the effects of radiation on the base temperature and that of radiative boundaries on the disturbance equations were neglected. Their results exhibit great improvement for the P_3 approximation over the P_1 approximation and less rapid improvement for the P_5 approximation. The same conclusion was also reached by Marshak[3] for the solution of the Milne problem in neutron transport theory.

The foregoing problems of a radiating gas solved with the P_3 approximation[11,12] neglected the effect of radiative boundaries caused by the presence of walls. Therefore, the boundary conditions required for the P_3 approximation were not needed. In what follows, the intensity of radiation relation in terms of the moments will be derived first. Then, the Marshak-type boundary conditions will be used to solve the equation of radiative transfer.

II. Angular Distribution of Radiation Intensity for P_3 Approximation

Consider a Cartesian coordinate system, as shown in Fig. 1, where $i = 1, 2, 3$. Therefore, the direction cosines are $\ell_1 = \cos\beta$, $\ell_2 = \sin\beta\cos\theta$, $\ell_3 = \sin\beta\sin\theta$, and the infinitesimal solid angle element is $d\Omega = \sin\beta\, d\beta d\theta$.

$\ell_1 = \ell_{x_1} = \cos\beta$

$\ell_2 = \ell_{x_2} = \sin\beta\cos\theta$

$\ell_3 = \ell_{x_3} = \sin\beta\sin\theta$

$\hat{u} = \cos\beta\,\hat{i} + \sin\beta\cos\theta\,\hat{j} + \sin\beta\sin\theta\,\hat{k}$

$d\Omega = \sin\beta\, d\beta\, d\theta = -d(\cos\beta)\, d\theta$

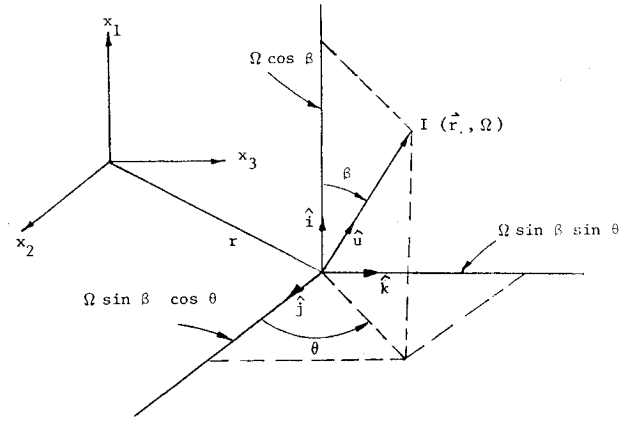

Fig. 1 Coordinate system showing intensity as a function of position and angle for Cartesian geometry.

The coefficients $A_\ell^m(r)$ in Eq. (1) are determined by taking the zeroth, first and third moments of Eq. (1) successively. These coefficients are listed in the Appendix. Introducing the normalized spherical harmonics in the Appendix, the P_3 approximation for intensity of radiation is obtained as:

$$\begin{aligned}
4\pi I(r,\Omega) &= I_0 + 3I_1 P_1^0(\cos\beta) + 3[I_2\cos\theta + I_3\sin\theta]P_1^1(\cos\beta) \\
&+ 5/2[3I_{11} - I_0]P_2^0(\cos\beta) + 5[I_{12}\cos\theta + I_{13}\sin\theta]P_2^1(\cos\beta) \\
&+ 5/4[2I_{23}\sin 2\theta - I_{33}\cos 2\theta]P_2^2(\cos\beta) + 7/2[5I_{111} - 3I_1] \\
&\times P_3^0(\cos\beta) + 7/4[(5I_{112} - I_2)\cos\theta + (5I_{113} - I_3)\sin\theta] \\
&\times P_3^1(\cos\beta) + 7/4[(2I_{22} - I_1)\cos 2\theta + 2I_{123}\sin 2\theta]P_3^2(\cos\beta) \\
&+ 7/2[(4I_{222} + 3I_{112} - 3I_2)\cos 3\theta \\
&- (4I_{333} + 3I_{113} - 3I_3)\sin 3\theta]P_3^3(\cos\beta)
\end{aligned} \tag{12}$$

A similar procedure can be followed in deriving the angular distribution of intensity relation in cylindrical and spherical coordinates. However, a simpler procedure is to convert Eq. (12) to cylindrical and spherical coordinates by using the transformation equations for tensors.

III. Boundary Conditions for P_3 Approximation

Consider a specularly and diffusely reflecting, diffusely emitting, opaque and gray boundary which is perpendicular to one of the Cartesian coordinates, e.g., x_1 direction in Fig. 1. The intensity of the radiation at this boundary is given as:

$$\begin{aligned}
I(x_2,x_3,0,\beta,\theta) &= \epsilon_w I_{bw} + \rho_{ws} I(x_2,x_3,0,\pi-\beta,\theta) \\
&+ \frac{\rho w d\int_0^{2\pi}\int_{\pi/2}^{\pi} I(x_2,x_3,0,\pi-\beta,\theta)\cos(\pi-\beta)\sin(\pi-\beta)\,d(\pi-\beta)}{\int_0^{2\pi}\int_{\pi/2}^{\pi}\cos(\pi-\beta)\sin(\pi-\beta)\,d(\pi-\beta)\,d\theta}
\end{aligned} \tag{13}$$

or

$$\begin{aligned}
i(x_2,x_3,0,\beta,\theta) &= \epsilon_w I_{bw} + \rho_{ws} I(x_2,x_3,0,\pi-\beta,\theta) \\
&+ \frac{\rho w d}{\pi}\int_0^{2\pi}\int_0^{\pi/2} I(x_1,x_2,0,\pi-\beta\theta)\cos\beta\sin\beta\, d\beta d\theta
\end{aligned} \tag{14}$$

where ϵ_w, ρ_{ws}, and ρ_{wd} are the emissivity, specular reflectivity, and diffuse reflectivity of the boundary, respectively, and I_{bw} is the black-body radiation intensity at the wall temperature. $I(x_2,x_3,0,\pi-\beta,\theta)$ is the total radiation intensity of the fluid adjacent to the wall in direction $(\pi-\beta,\theta)$ obtained by integrating overall wavelengths. Obviously, on the right-hand side of this equation, the explicit form of the angular distribution of radiation intensity is given by Eq. (12) in terms of the moments. The boundary conditions needed for the P_3 approximation for a three-dimensional geometry can be adapted from Marshak.[3] Marshak's boundary condition is generalized as

$$\int_{\cup} I_w(r,\Omega)\gamma_i^{n-1}\,d\Omega = \int_{\cup} f\gamma_i^{2n-1}\,d\Omega \tag{15}$$

where $\cup$ and $\cap$ indicate the integrations over the appropriate half-solid angles, $d\Omega$ is the infinitesimal solid-angle element, $n=1$, 2 for the P_3 approximation, and $i=1,2,3$ for a three-dimensional Cartesian geometry.

The application of the Marshak's boundary condition to Eq. (14) with the angular distribution of the intensity $I(r,\Omega)$ as given by Eq. (12) yields

$$3I_0 \pm 16(1+2\xi)I_i + 15I_{ii} = 32E_{bw}$$

$$-(2+5\lambda)I_0 \pm 16\lambda I_i + 15(2+\lambda)I_{ii} \pm \tag{16}$$

$$32(1+2\xi-\lambda)I_{iii} = 32E_{bw} \tag{17}$$

where

$$\xi = (1-\epsilon_w)/\epsilon_w \quad \text{and} \quad \lambda = \rho_{wd}/\epsilon_w \tag{18}$$

and + or − signs indicate the respective boundary facing in the positive and negative x direction and $i=1,2,3$.

IV. Solutions to the Equation of Radiative Transfer by Spherical Harmonics Method

To illustrate the P_3 approximation with its developed boundary conditions, the one-dimensional pure radiation heat transfer between boundary surfaces with known temperature, specifically plane parallel plates, concentric cylinders, and concentric spheres will be considered. The physical model and its associated coordinate systems are shown in Figs. 1 and 2. The walls are considered to be isothermal, gray diffuse emitters, and diffuse and specular reflectors. The space between the walls is filled with a homogeneous, absorbing, emitting, and gray medium without any heat generation. The net radiative heat flux is calculated and the results are compared with the other approximate and exact solutions.

Plane Parallel Plates

If the boundary conditions for the governing transfer equation are independent of the azimuthal angle, the radiation intensity becomes a function of x_1 and the polar angle for the one-dimensional Cartesian geometry. Both the governing transfer equation and moment differential equation are deduced from Eqs. (3-11) by letting $i=j=k=1$. Defining an optical thickness $\tau=\alpha x_1$, one obtains

$$\frac{dI_I}{d\tau} = E_b - I_0 \tag{19a}$$

$$\frac{dI_{II}}{d\tau} = -I_I \tag{19b}$$

$$\frac{dI_{III}}{d\tau} = \frac{4}{3}E_b - I_{II} \tag{19c}$$

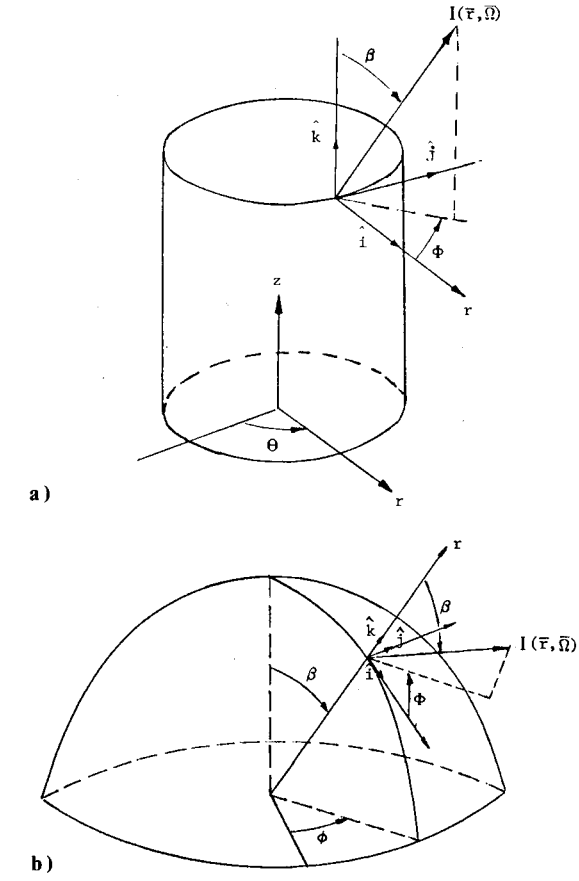

Fig. 2 Coordiante system: a) cylindrical geometry, b) spherical.

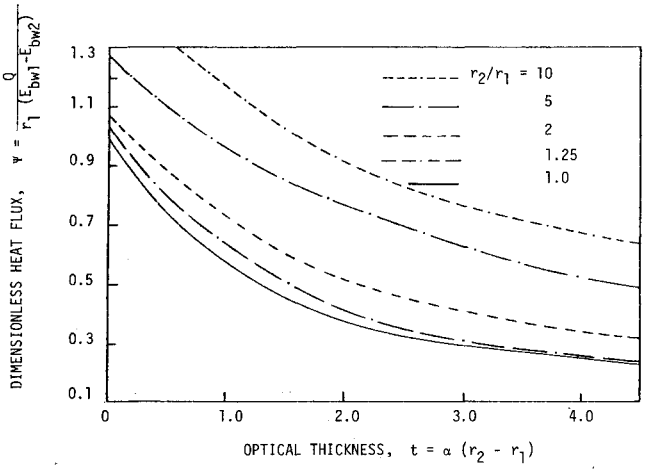

Fig. 3 Effect of radius ratio on the energy transfer between infinitely long, concentric black cylinders.

$$\frac{dI_{IIII}}{d\tau} = -I_{III} \tag{19d}$$

$$I_{IIII} = \frac{6}{7}I_{II} - \frac{3}{35}I_0 \tag{19e}$$

For the fluid in radiative equilibrium, the first moment of intensity I_1 is the heat transfer through the medium Q, and the zeroth moment of intensity I_0 is equal to $4E_b$. Therefore, differentiation and backward substitution of Eq. (19) yields

$$I_I = -\frac{1}{3}\frac{dI_0}{d\tau} + \frac{3}{35}\frac{d^2I_0}{d\tau^2} \tag{20a}$$

and

$$\frac{d^4 I_0}{d\tau^4} - \frac{35}{9}\frac{d^2 I_0}{d\tau^2} = 0 \tag{20b}$$

The solution to Eq. (20b) is:

$$I_0 = A_1 + A_2\tau + A_3\cosh(\sqrt{35}/3)\tau + A_4\sinh(\sqrt{35}/3)\tau \tag{21}$$

where constants A_1, A_2, A_3, and A_4 are found using boundary conditions defined by Eqs. (16-18) for $i=1$. Note that I_{II} and I_{III} can be expressed in terms of I_0 and its derivatives by use of Eq. (19), and Eqs. (20) yield $I_1 = -(1/3)A_2$. Therefore, a dimensionless heat flux ψ can be evaluated as

$$\psi = \psi_{p_3} = Q/(E_{bw_1} - E_{bw_2}) \tag{22}$$

where E_{bw_1} and E_{bw_2} are the black-body emissive powers of the boundaries. Similar work can be found in Özisik[8] for the P_1 approximation and the dimensionless heat flux is given as:

$$\psi_{p_1} = 1/(\tfrac{3}{4}\tau + \xi_1 + \tfrac{1}{2} + \xi_2 + \tfrac{1}{2}) \tag{23}$$

where $\xi = (1-\epsilon)/\epsilon$.

It is observed that while ψ_{p_1} is independent of boundary emissive powers E_{bw_1} and E_{bw_2}, ψ for the P_3 approximation depends on E_{bw_1} and E_{bw_2}. The variation of the dimensionless heat flux with optical thickness is plotted in Fig. 3, which corresponds to the case $r_2/r_1 \to 1$ of the concentric cylinder solution. There is a negligible difference between the P_1 and P_3 approximations for plane parallel plates. Consequently, only one curve was drawn in Fig. 3 to represent both cases. The P_1 approximation is equivalent to assuming isotropy for the intensity of radiation. The P_3 approximation modifies the isotropy assumption. For parallel plates, the intensity distribution is semi-isotropic, making the assumption of isotropy a fair approximation. Hence, the modification afforded by P_3 does not alter the solution by a significant factor. Both the P_1 and P_3 approximations reduce to the classical shape factor when the optical thickness is zero.

Concentric Cylinders

For cylindrical symmetry, the radiation intensity is a function in radius r, polar angle β, and azimuthal angle ϕ. The governing equation[8,14] is:

$$\sin\beta\left[\cos\phi\frac{\partial I}{\partial\tau} - \frac{\sin\phi}{\tau}\frac{\partial I}{\partial\phi}\right] + I = I_b \tag{24}$$

where $\tau = \alpha r$ is the optical thickness.

The moment-differential equations are developed by multiplying Eq. (33) by $(\sin\beta\ \cos\phi)^n$ for $n=0,1,2,3$ and integrating over a solid angle of 4π, and noting that the second term on the left-hand side of Eq. (33) is integrated by parts. The first four moment equations are:

$$\frac{1}{\tau}\frac{d}{d\tau}(\tau I_r) + I_0 = E_b \tag{25}$$

$$\frac{1}{\tau^2}\frac{d}{d\tau}(\tau^2 I_{rr}) + I_r - \frac{1}{\tau}\int_\Omega I\sin^2\beta\, d\Omega = 0 \tag{26a}$$

$$\frac{1}{\tau^3}\frac{d}{d\tau}(\tau^3 I_{rrr}) + I_{rr} - \frac{2}{\tau}\int_\Omega I\sin^3\beta\cos\phi\, d\Omega = \frac{4}{3}E_b \tag{26b}$$

$$\frac{1}{\tau^4}\frac{d}{d\tau}(\tau^3 I_{rrrr}) + I_{rrr} - \frac{3}{\tau}\int_\Omega I\sin^4\beta\cos^2\phi\, d\Omega = 0 \tag{26c}$$

where $E_b = \pi I_b$.

In order to evaluate the integral terms, the P_3 expansion for the intensity is substituted into Eqs. (26) with the assumption of the isotropy of intensity only in the evaluation of the preceding integrals. Then, Eqs. (26) reduce to:

$$\frac{1}{\tau^2}\frac{d}{d\tau}(\tau^2 I_{rr}) + I_r - \frac{2}{3\tau}I_0 = 0 \tag{27a}$$

$$\frac{1}{\tau^3}\frac{d}{d\tau}(\tau^3 I_{rrr}) + I_{rr} - \frac{8}{5\tau}I_r = \frac{4}{3}E_b \tag{27b}$$

$$\frac{1}{\tau^4}\frac{d}{d\tau}(\tau^4 I_{rrrr}) + I_{rrr} - \frac{3}{\tau}\left(\frac{32}{35}I_{rr} - \frac{4}{105}I_0\right) = 0 \tag{27c}$$

Equations (25) and (27) contain six unknowns, making it necessary to obtain two more equations. When I_{rrrr} is evaluated, the closure condition is:

$$I_{rrrr} = \int I\sin^4\beta\cos^4\phi\, d\Omega = \frac{6}{7}I_{rr} - \frac{3}{35}I_0 \tag{28}$$

The conservation of thermal energy

$$\frac{d}{dr}(rI_0) = 0 \tag{29}$$

yields $I_r = Q/r = \alpha Q/\tau$ and $I_0 = 4E_b$. Therefore, combining Eqs. (27-29) gives

$$I_r = -\left(\frac{1}{3} + \frac{3}{35\tau^2}\right)\frac{dI_0}{d\tau} + \frac{3}{35\tau}\frac{d^2 I_0}{d\tau^2} + \frac{3}{35}\frac{d^3 I_0}{d\tau^3} \tag{30a}$$

$$I_{rr} = \frac{1}{3}I_0 - \left(\frac{23}{105\tau} + \frac{96}{1225\tau^3}\right)\frac{dI_0}{d\tau} - \left(\frac{3}{35} - \frac{96}{1225\tau^2}\right)\frac{d^2 I_0}{d\tau^2} + \frac{96}{1225\tau}\frac{d^3 I_0}{d\tau^3} \tag{30b}$$

$$I_{rrr} = -\left(\frac{1}{5} + \frac{366}{1225\tau^2} + \frac{3456}{42875\tau^4}\right)\frac{dI_0}{d\tau} - \left(\frac{18}{1225\tau} - \frac{3456}{42375\tau^3}\right)\frac{d^2 I_0}{d\tau^2} + \left(\frac{18}{245} + \frac{3456}{42875\tau^2}\right)\frac{d^3 I_0}{d\tau^3} \tag{30c}$$

and

$$\frac{d^4 I_0}{d\tau^4} + \frac{2}{\tau}\frac{d^3 I_0}{d\tau^3} - \left(\frac{35}{9} + \frac{1}{\tau^2}\right)\frac{d^2 I_0}{d\tau^2} - \left(\frac{35}{9\tau} - \frac{1}{\tau^3}\right)\frac{dI_0}{d\tau} = 0 \tag{30d}$$

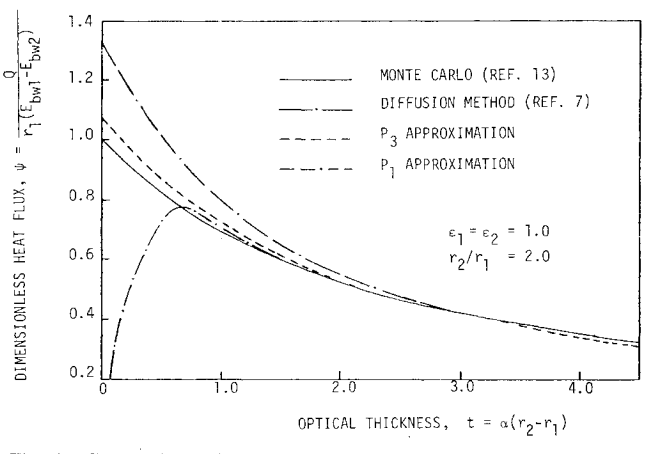

Fig. 4 Comparison of solutions of energy transfer between infinitely long, concentric black cylinders.

Applying Marshak's boundary condition, as in Eq. (15), to the diffusely and specularly reflecting and diffusely emitting boundaries of this cylindrical geometry, the following boundary conditions are obtained:

$$3I_0 \pm 16(1+2\xi)I_r + 15I_{rr} = 32E_{bw} \tag{31a}$$

$$-(2+5\lambda)I_0 \pm 16\lambda I_r + 15(2+\lambda)I_{rr}$$

$$\pm 32(1-\lambda+2\xi)I_{rrr} = 32E_{bw} \tag{31b}$$

where + and − indicate the inner and outer boundaries of the concentric cylinder, respectively, while ξ and λ are as defined in Eq. (18).

Equation (30d) can be solved numerically using boundary conditions given in Eqs. (31). The dimensionless heat flux ψ is obtained as:

$$\psi_{P_3} = Q/[r_1(E_{bw_1} - E_{bw_2})] = I_r(\tau_1)/(E_{bw_1} - E_{bw_2})$$

$$= \frac{1}{E_{bw_2} - E_{bw_1}}\left[-\left(\frac{1}{3} + \frac{3}{35\tau^2}\right)\frac{\partial I_0}{\partial \tau} + \frac{3}{35}\frac{\partial^2 I_0}{\partial \tau^3}\right]\Bigg|_{\tau=\tau_1} \tag{32}$$

which is a function of $\tau_1, \tau_2, E_{bw1}, E_{bw2}, \xi_1, \xi_2, \lambda_1$, and λ_2. A new independent variable t may be defined as $t = \alpha(r_2 - r_1) = \tau_2 - \tau_1$; further, let $p = r_2/r_1$. Then, for given values of $t, p, E_{bw1}, E_{bw2}, \xi_1, \xi_2, \lambda_1, \lambda_2, \psi_{P_3}$ can be calculated numerically. Following a similar procedure for the P_1 approximation would give

$$\psi_{P_1} = 1\Big/\left[\frac{3}{4}\frac{t}{p-1}\ln p + \xi_1 + \frac{1}{2} + \frac{1}{p}\left(\xi_2 + \frac{1}{2}\right)\right] \tag{33}$$

The comparison of dimensionless heat flux for different radii ratios with optical thickness is given in Fig. 3. Figure 4 depicts results for a concentric cylinder whose radii ratio is 2. There is a great improvement for the P_3 approximation compared to the P_1 and diffusion approximations in the thin gas region. In the limiting case of zero optical thickness, the respective overestimates of heat flux by the P_3, P_1, and diffusion approximations are about 8%, 33%, and −100% compared to the Monte Carlo method.

The intensity distribution for a concentric cylinder is piecewise isotropic, but the P_1 approximation assumes intensity to be isotropic. The P_3 approximation is better because the isotropy assumption is modified. Since the resulting modification does not make the intensity distribution piecewise isotropic, the P_3 approximation remains inferior to the Monte Carlo method. However, the cost of P_3 approximation may make it useful where a maximum overestimate of about 10% is expected. The variation of dimensionless heat flux for different surface emissivities are shown in Fig. 5.

Concentric Spheres

In a medium with spherical symmetry, the radiation intensity is a function of radius r and angle θ between the radius vector and intensity beam. The governing equation is:

$$\mu\frac{dI}{d\tau} + \frac{1-\mu^2}{\tau}\frac{dI}{d\mu} + I(\tau,\mu) = I_b \tag{34}$$

where $\mu = \cos\theta$ and $\tau = \alpha r$.

The differential equations in terms of moments are obtained by multiplying Eq. (34) by μ^n and integrating over a solid angle of 4π. For $n = 0,1,2,3$,

$$\frac{1}{\tau^2}\frac{d}{d\tau}(\tau^2 I_r) + I_0 = 4E_b \tag{35a}$$

$$\frac{1}{\tau^3}\frac{d}{d\tau}(\tau^3 I_{rr}) + I_r - \frac{I_0}{\tau} = 0 \tag{35b}$$

$$\frac{1}{\tau^4}\frac{d}{d\tau}(\tau^4 I_{rrr}) + I_{rr} - \frac{2I_r}{\tau} = \frac{4}{3}E_b \tag{35c}$$

$$\frac{1}{\tau^4}\frac{d}{d\tau}(\tau^5 I_{rrrr}) + I_{rrr} - \frac{3I_{rr}}{\tau} = 0 \tag{35d}$$

From conservation of thermal energy, $I_r = \alpha^2 Q/\tau^2$ and $I_0 = 4E_b$. Following the same procedure of concentric cylinder geometry and using the angular distribution of intensity, the closing condition is evaluated as:

$$I_{rrrr} = \frac{6}{7}I_{rr} - \frac{3}{35}I_0 \tag{36}$$

and the governing equation results

$$\frac{d^4 I_0}{d\tau^4} + \frac{4}{\tau}\frac{d^3 I_0}{d\tau^3} - \frac{35}{9}\frac{d^2 I_0}{d\tau^2} - \frac{70}{9\tau}\frac{dI_0}{d\tau} = 0 \tag{37}$$

Marshak's boundary conditions for spherical geometry are obtained similarly to those in Cartesian and cylindrical coordinates by using an appropriate intensity function in terms of I_0, I_r, I_{rr}, and I_{rrr}. Then, these equations are expressed in terms of I_0 and its first three derivatives with respect to τ. A numberical solution to Eq. (37) has been obtained and the dimensionless heat flux is plotted in Fig. 6.

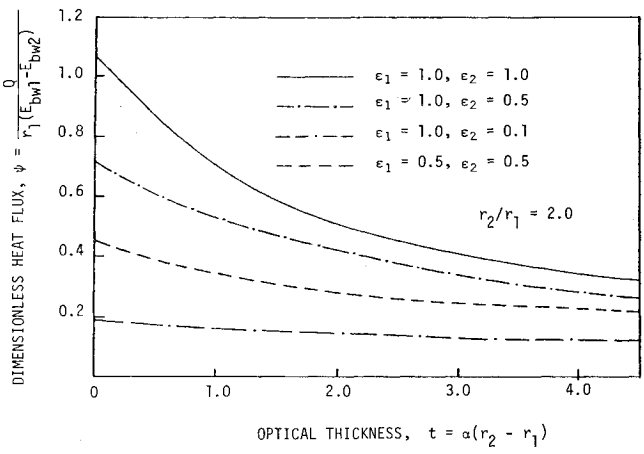

Fig. 5 Effect of wall emissivities on the energy transfer between infinitely long, concentric gray cylinders.

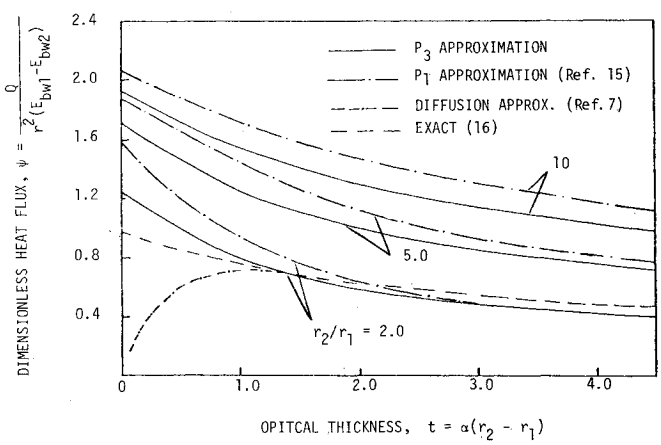

Fig. 6 Comparison of solutions of energy transfer between concentric spheres.

The dimensionless heat flux in this figure is:

$$\Psi_{p_3} = \frac{Q}{r_1^2(E_{bw_1} - E_{bw_2})} = \frac{I_r(\tau_1)}{E_{bw_1} - E_{bw_2}} \tag{38}$$

Figure 6 also includes the dimensionless heat flux obtained by Dennar and Sibulkin[15] as:

$$\Psi_{p_1} = 1 \Big/ \left[\frac{\sqrt{3}}{2} \tau_1 \left(1 - \frac{r_1}{r_2}\right) + \left(\left(\frac{1}{\epsilon_1} - \frac{1}{2} \right) + \frac{1}{\epsilon_2} - \frac{1}{2} \right) \frac{r_1^2}{r_2^2} \right] \tag{39}$$

The results for concentric spheres in Fig. 6 contain a curve for exact solution by Ryhming,[16] for radii ratio of 2.0. Considering the thin gas region, P_3 is observed to be better than P_1 and diffusion approximations for zero optical thickness. The P_3 and P_1 approximations overestimate the heat flux by about 25 and 60%, respectively, when the radii ratio is two. As in concentric cylinders, the intensity distribution for concentric spheres is piecewise isotropic and exact solutions account for such a distribution. P_1 assumes isotropic intensity, while P_3 modifies the isotropy assumption resulting in better solutions.

V. Comparison of P_3 Approximation With Other Modified Methods

It is observed that the shortcoming of the first-order approximation is the assumption of a near isotropic intensity distribution. Such an approximation gives acceptable results in three cases: when the medium is optically thick, when radiation intensity is due to the source term with walls at the same temperature, and for a Cartesian geometry where the intensity is semi-isotropic.

For cylindrical and spherical geometries, the curvature effects make the intensity distribution piecewise isotropic. The exact treatment of radiative transfer will automatically account for nonplanar effects. However, by modifying or improving on the P_1 approximation, the effects of curvature can be either eliminated or minimized. Modest and Stevens[17] used the P_1 approximation and exact treatment to obtain geometric factors which improve the results. Olfe[18] obtained good results by analyzing the surface emissive power contribution exactly while utilizing P_1 approximation for the gas

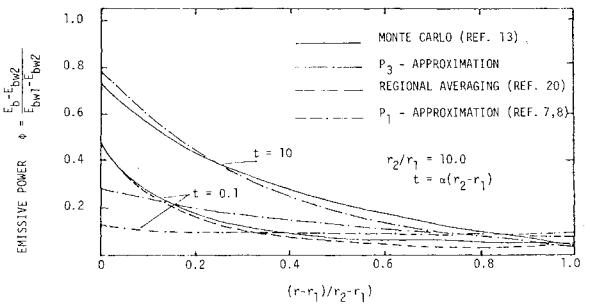

Fig. 7 Distribution of gas emissive power between concentric cylinders.

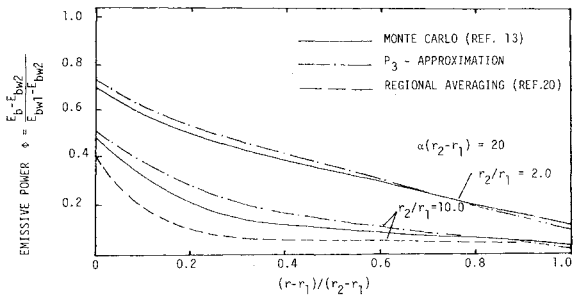

Fig. 8 Distribution of gas emissive power between concentric emissive power.

emission contribution. Chou and Tien[19] approached the problem by dividing the radiation field into solid-angle subregions and approximating the moments of intensity by their mean values. The subdivision accounts for the curvature effects giving better results.

The preceding modifications share one advantage over the P_3 approximation. They give good results, compared to exact solutions, for the whole range of optical thickness. For comparison purposes, emissive power distribution (Figs. 7 and 8) and heat flux to the inner wall (Tables 1 and 2) are shown for a cylinder. Tables 1 and 2 reveal that the accuracy of the P_3 approximation is limited to lower radius ratios ($r_2/r_1 \sim 2$) for thin optical thicknesses, while modified

Table 1 Comparison of methods for dimensionless heat transfer to the inner wall of cylinder, $r_1/r_2 = 10$

Optical thickness	Method					
	Exact[13]	Modified[19]	Regional[20]	P_1 approx.	P_3 approx.	Diffusion[7,21]
0.0	1.00	1.00	1.00	1.811	1.54	0.0
0.1	0.982	0.982	1.031	1.757	1.48	0.025
0.2	0.964	0.964	1.074	1.700	1.44	0.055
0.5	0.941	0.941	1.105	1.548	1.33	0.211
1.0	0.882	0.880	1.105	1.348	1.16	0.400
2.0	0.776	0.768	0.884	1.071	0.917	0.564
5.0	0.564	0.547	0.652	0.663	0.605	0.529

Table 2 Comparison of methods for dimensionless heat transfer to the inner wall of cylinder, $r_1/r_2 = 2.0$

Optical thickness	Method					
	Exact[13]	Modified[19]	Regional[20]	P_1 approx.	P_3 approx.	Diffusion[7,21]
0.0	1.000	1.00	1.00	1.333	1.08	0.0
0.1	0.960	0.960	0.960	1.247	1.03	0.220
0.2	0.925	0.925	0.925	1.171	0.982	0.397
0.5	0.829	0.810	0.810	0.990	0.805	0.726
1.0	0.685	0.680	0.680	0.787	0.710	0.705
2.0	0.528	0.521	0.521	0.559	0.535	0.535
6.0	0.257	0.257	0.257	0.258	0.251	0.254

methods compare favorably with exact solution. Despite the increased accuracy, the modifications introduce some integral expressions which remove the element of simplicity afforded by the P_3 and P_1 approximations.

In spite of its limited accuracy, the P_3 approximation does have three advantages: easy incorporation of scattering effects, straight-forward extension to two-dimensional problems, and solutions that can be obtained by standard techniques. With the exception of work in Ref. 17, other modifications have not been extended to multidimensional problems. While such an extension may be feasible, it is likely to be more cumbersome than that of the P_3 approximation. In cases where radiation, conduction, convection, and combustion are coupled, the P_3 approximation may be more convenient than the modified forms because of the differential nature of the mentioned coupling effects.

For pure radiation in one-dimensional problems, accuracy requirements may dictate use of exact or modified solutions. However, for heat transfer coupled with multidimensional problems, the complexities may render the P_3 approximation a better approach, especially in instances where the P_1 approximation is being used.

IV. Discussion

In this paper, an absorbing, emitting and gray medium is considered. Following the ideas discussed by Traugott,[21] the present analysis can be modified to include the weighted effects of the nongrayness of the fluid by defining a nongrayness factor $\eta=(\alpha_p/\alpha_R)^{1/2}$, where α_p and α_R are Planck mean and Rosseland mean coefficients, respectively.

Since suspended particles present in the medium, depending on their range of size distribution and the concentration, may have important effects on the radiation, the analysis can easily be extended to include the effect of isotropically scattering fluid in terms of a single scattering albedo, $\omega=\sigma/(\alpha_p+\sigma)$, where σ is the mean scattering coefficient.

Although the solutions to one-dimensional problems are presented to demonstrate the convenience and effectiveness of the formulations, it is quite general. It can be extended to solve problems of multidimensional geometry which have been solved by the P_1 approximation and where further accuracy is needed.

Likewise, when radiation is coupled with convection and/or conduction, the exact treatment of the problem becomes a nonlinear integrodifferential equation. The mathematical complexity associated with nonlinearity of the approximate differential equation by the P_3 formulation remains, but the complexity of its being an integrodifferential equation is uncompounded.

It is observed that the shortcoming of the first-order approximations is the assumption of isotropic intensity distribution. This may be corrected by use of higher order approximations which tend to modify the isotropic distribution of intensity. One would therefore expect better results if the P_3 approximation were used.

Appendix

The coefficients $A_l^m(r)$ in Eq. (1) can be determined by taking the zeroth, first, second, and third moments of Eq. (1), successively. The list of $A_l^m(r)$ is:

$$A_0^0=\frac{1}{2\sqrt{\pi}}I_0,\quad A_1^0=\frac{1}{2}\sqrt{\frac{3}{\pi}}I_1,\quad A_1^{-1}=\frac{1}{2}\sqrt{\frac{3}{2\pi}}(I_1+iI_3)$$

$$A_1^1=\frac{1}{2}\sqrt{\frac{3}{2\pi}}(I_2+iI_3),\quad A_2^0=\frac{1}{4}\sqrt{\frac{5}{\pi}}(3I_{11}-I_0)$$

$$A_2^{-1}=\frac{1}{2}\sqrt{\frac{15}{2\pi}}(I_{12}+iI_{13}),\quad A_2^1=\frac{1}{2}\sqrt{\frac{15}{2\pi}}(I_{12}-iI_{13})$$

$$A_2^{-2}=\frac{1}{2}\sqrt{\frac{15}{2\pi}}(6I_{22}+3I_{11}-3I_0+iI_{23})$$

$$A_2^2=\frac{1}{2}\sqrt{\frac{15}{2\pi}}(6I_{22}+3I_{11}-3I_0-iI_{23})$$

$$A_3^0=\frac{1}{4}\sqrt{\frac{7}{\pi}}(5I_{111}-3I_1)$$

$$A_3^{-1}=\frac{1}{8}\sqrt{\frac{21}{\pi}}(5I_{112}-I_2+i5I_{113}-iI_3)$$

$$A_3^1=\frac{1}{8}\sqrt{\frac{21}{\pi}}(5I_{112}-I_2-i5I_{113}+iI_3)$$

$$A_3^{-2}=\frac{1}{4}\sqrt{\frac{105}{2\pi}}(2I_{122}+I_{111}-I_1+iI_{123})$$

$$A_3^2=\frac{1}{4}\sqrt{\frac{105}{2\pi}}(2I_{122}+I_{111}-I_1-iI_{123})$$

$$A_3^{-3}=\frac{1}{8}\sqrt{\frac{35}{\pi}}(4I_{222}+3I_{112}-3I_2-i4I_{333}+i3I_{113}+i3I_3)$$

$$A_3^3=\frac{1}{8}\sqrt{\frac{35}{\pi}}(4I_{222}+3I_{112}-3I_2+i4I_{333}+i3I_{113}-iI_3)\qquad\text{(A1)}$$

with the following additional relations:

$$I_0=I_{11}+I_{22}+I_{33},\quad I_1=I_{111}+I_{122}+I_{133}$$

$$I_2=I_{211}+I_{222}+I_{233},\quad I_3=I_{311}+I_{322}+I_{333}\qquad\text{(A2)}$$

References

[1] Jeans, J. H., "The Equations of Radiative Transfer of Energy," *Monthly Notices of Royal Astronomical Society*, Vol. 78, Nov. 1917, pp. 28-36.

[2] Mark, J. C., "The Spherical Harmonics Method," Parts I and II, National Research Council of Canada, Atomic Energy Repts. No. MT 92 (1944) and MT 97 (1945).

[3] Marshak, R. E., "Note on the Spherical Harmonics Method as Applied to the Milne Problem for a Sphere," *Physical Review*, Vol. 71, April 1947, pp. 443-446.

[4] Pelland, B., "Numerical Comparison of Different Types of Vacuum Boundary Conditions for the P_n Approximation," *Transactions of American Nuclear Society*, Vol. 9, 1966, pp. 434-435.

[5] Schmidt, E. and Gelbard, E. M., "A Double P_n Method for Spheres and Cylinders," *Transactions of American Nuclear Society*, Vol. 9, 1966, pp. 432-433.

[6] Krook, M., "On the Solutions of Equation of Transfer, I," *Astrophysical Journal*, Vol. 122, Nov. 1955, pp. 488-497.

[7] Siegel, R. and Howell, J. R., *Thermal Radiation Heat Transfer*, McGraw-Hill, New York, 1972.

[8] Özisik, N. M., *Radiative Transfer*, John Wiley & Sons, New York, 1973.

[9] Spiegel, E. A., "The Smoothing of Temperature Fluctuations by Radiative Transfer," *Astrophysical Journal*, Vol. 126, July 1957, pp. 202-207.

[10] Unno, W. and Spiegel, E. A., "The Eddington Approximation in the Radiative Heat Equation," *Publications of the Astronomical Society of Japan*, Vol. 18, March 1966, pp. 85-95.

[11] Arpaci, V. S. and Gözüm, D., "Thermal Stability of Radiating Fluids: The Benard Problem," *The Physics of Fluids*, Vol. 16, May 1973, pp. 581-588.

[12] Spiegel, E. A., "The Convective Instability of a Radiating Fluid Layer," *Astrophysical Journal*, Vol. 132, Nov. 1960, pp. 716-728.

[13] Permutter, M. and Howell, J. R., "Radiant Transfer through a Gray Gas between Concentric Cylinders using Monte Carlo," *Journal of Heat Transfer*, Vol. 86, Feb. 1964, pp. 165-179.

[14]Uesugi, A. and Tsujita, J., "Diffuse Reflection of a Searchlight Beam by Slab, Cylindrical and Spherical Media," *Publications of the Astronomical Society of Japan*, Vol. 21, Oct. 1969, pp. 370.

[15]Dennar, E. A. and Sibulkin, M., "An Evaluation of the Differential Approximation for Spherically Symmetric Radiative Transfer," American Society of Mechanical Engineers Paper 68-HT-21, Sept. 1968.

[16]Ryhming, I. L., "Radiative Transfer between Two Concentric Spheres Separated by an Absorbing and Emitting Gas," *International Journal of Heat and Mass Transfer*, Vol. 9, March 1966, pp. 199-206.

[17]Modest, M. F. and Stevens, D. S., "Two Dimensional Radiative Equilibrium of a Gray Medium between Concentric Cylinders," *Journal of Quantitative Spectroscopy and Radiative Transfer*, Vol. 19, 1978, pp. 353-365.

[18]Olfe, D. B., "Application of the Modified Differential Approximation to Radiative Transfer in a Gray Medium between Concentric Cylinders and Spheres," *Journal of Quantitative Spectroscopy and Radiative Transfer*, Vol. 8, March 1968, pp. 899-907.

[19]Chou, Y. S. and Tien, C. L., "A Modified Moment Method for Radiative Transfer in Non-planar Systems," *Journal of Quantitative Spectroscopy and Radiative Transfer*, Vol. 8, March 1968, pp. 919-933.

[20]Deissler, R. G., "Diffusion Approximation for Thermal Radiation in Gases with Jump Boundary Conditions," *Journal of Heat Transfer*, Vol. 86C, May 1964, pp. 240-246.

[21]Traugott, S. C., "Radiative Heat-Flux Potential for a Nongray Gas," *AIAA Journal*, Vol. 4, March 1966, pp. 541-542.